J. Fluid Mech. (1994), *vol.* 270, *pp.* 175–198

Bounds for threshold amplitudes in subcritical shear flows

By GUNILLA KREISS[1], ANDERS LUNDBLADH[2] AND DAN S. HENNINGSON[2]

[1] Department of Numerical Analysis and Computer Science, Royal Institute of Technology, S-100 44 Stockholm, Sweden

[2] Department of Mechanics, Royal Institute of Technology, S-100 44 Stockholm, Sweden *and* The Aeronautical Research Institute of Sweden (FFA), Box 11021, S-161 11 Bromma, Sweden

(Received 27 April 1993 and in revised form 28 December 1993)

A general theory which can be used to derive bounds on solutions to the Navier–Stokes equations is presented. The behaviour of the resolvent of the linear operator in the unstable half-plane is used to bound the energy growth of the full nonlinear problem. Plane Couette flow is used as an example. The norm of the resolvent in plane Couette flow in the unstable half-plane is proportional to the square of the Reynolds number (R). This is now used to predict the asymptotic behaviour of the threshold amplitude below which all disturbances eventually decay. A lower bound is found to be $R^{-21/4}$. Examples, obained through direct numerical simulation, give an upper bound on the threshold curve, and predict a threshold of R^{-1}. The discrepancy is discussed in the light of a model problem.

1. Introduction

Stability of flows to finite-amplitude disturbances has been the focus of numerous investigations. For parameter values allowing linear instability all perturbations, save for a few fulfilling certain symmetries, will lead to sustained non-vanishing solutions. On the other hand, for other parameter values it is possible to show that all disturbances vanish in some suitable metric. In between these values, in what for shear flows is called the subcritical Reynolds-number regime, the stability depends both on the form and the amplitude of the perturbation. Here, very few results pertinent to anything but specific disturbances are available.

The Reynolds–Orr equation, which describes the evolution of the disturbance energy with respect to a base flow satisfying the incompressible Navier–Stokes equations (Reynolds 1895; Orr 1907), shows that the smallest Reynolds number for which energy growth may occur is independent of the amplitude. This equation was used by Serrin (1959) to prove that below the Reynolds number 5.71 (based on the maximum velocity of the base flow and the maximum diameter of the domain) all disturbances exhibit monotonic decay of the energy. Similar results were shown for geometries where the flow domain was bounded in at least one direction. Applying the same approach Joseph (1966) derived the exact lower limit on Reynolds number for disturbance energy growth in plane Couette flow. This theory can be extended to other parallel shear flows, as well as flows satisfying the Boussinesq equations for thermal convection (Joseph 1976). We will denote the critical parameter value given by this energy theory as R_E.

For Bénard convection in the Boussinesq approximation and with non-slip boundary conditions, Joseph (1965) showed that R_E coincides with the critical Rayleigh number

(R_L) for growth of eigenmodes of the linearized problem. In what follows R_L may denote either this critical Rayleigh number or the corresponding critical Reynolds number. Davis (1969) found that R_L differed from R_E if the problem has a free surface with surface tension and that the difference could be changed by varying the surface tension parameter. He found that R_E was determined from the self-adjoint part of the linear operator. This is in general true for problems with nonlinearities arising from the convective terms (Galdi & Straughan 1985). Reddy & Henningson (1993) pointed out that the linear operator need not be self-adjoint for $R_E = R_L$, but that a sufficient condition for this to hold is that it is normal, i.e. that it commutes with its adjoint. For parallel shear flows the non-normality of the linear operator increases exponentially with the Reynolds number† (Reddy, Schmid & Henningson 1993) and R_E and R_L may be separated by more than two orders of magnitude, as for example for plane Poiseuille flow. R_L may also approach infinity, as is the case in plane Couette flow (Romanov 1973; Herron 1991). For problems governed by non-normal operators with a subcritical Reynolds number range ($R_E < R < R_L$) few nonlinear stability results exist.

In the subcritical Reynolds-number regime it has been shown that solutions to the linearized problem may experience growth. For parallel shear flows this transient energy growth scales with the square of the Reynolds number and can take on large values before the decay predicted by the eigenvalues sets in (Gustavsson 1991; Butler & Farrell 1992; Reddy & Henningson 1993). The disturbances that experience maximum growth rates are streamwise vortices which in Fourier space are associated with low streamwise wavenumbers.

Recent numerical simulations of transition in plane Poiseuille flow (Henningson, Lundbladh & Johansson 1993; Schmid & Henningson 1992) show that the mechanism responsible for the subcritical growth may also supply finite-amplitude disturbances with energy. The energy gain that occurs in Fourier components with small streamwise wavenumbers is transferred to larger wavenumbers, rapidly making the flow turbulent. In fact, it follows from the Reynolds–Orr equation that the total disturbance energy can only grow from the effect of the linearized operator and that the nonlinear terms solely transfer energy among the wavenumbers.

One of the conventional ways of assessing the nonlinear properties of systems of dynamical equations is to follow stationary solutions. For Bénard convection Gor'kov (1957) and Malkus & Veronis (1958) independently found steady nonlinear solutions close to the linearly critical Rayleigh number. Since $R_E = R_L$ in this flow, the bifurcation from the null solution into the finite-amplitude state is supercritical and the predicted solutions are in general stable, allowing them to be observed experimentally. For parallel shear flows Stuart (1960) and Watson (1960) derived the Landau equation, valid close to R_L, and showed that the bifurcation is subcritical. Herbert (1983) reviewed weakly nonlinear theory and showed that the radius of convergence of such expansions in shear flows is prohibitively small.

Solutions to the nonlinear problem can also be found directly without assuming that the amplitude is small. For two-dimensional disturbances in plane Poiseuille flow Meksyn & Stuart (1951), using an approximate method, demonstrated that two-dimensional waves of finite amplitude are unstable down to a Reynolds number about half of the linearly critical one. Based on these results Grohne (1969) and Zahn *et al.*

† A normal operator or matrix has orthogonal eigenfunctions. The condition number of the matrix containing the normalized eigenvectors as column vectors thus has the value one. For non-normal matrices the condition number is greater than one and can be used as a measure of non-normality. An operator can be projected onto an appropriate finite-dimensional subspace where the same measure of non-normality may be used.

(1974) numerically calculated two-dimensional and some three-dimensional steady-state finite-amplitude solutions. The latter being a rather computationally intensive task, only recently have more accurate steady three-dimensional finite-amplitude solutions for this flow become available (Ehrenstein & Koch 1991).

Since R_L approaches infinity for plane Couette flow, weakly nonlinear solutions are not possible, and apparently neither are steady two-dimensional solutions (Cowley & Smith 1985). Nagata (1990), however, has provided three-dimensional finite-amplitude solutions by starting with Taylor–Couette flow in the narrow-gap approximation, and letting the system rotation vanish.

Apart from the energy methods, results for general disturbances can be derived by considering the resolvent of the linearized operator, i.e. the solution operator of the Laplace-transformed problem. In this way Romanov (1973) proved nonlinear stability of plane Couette flow, and Yudovich (1989) established the decay of solutions of the Navier–Stokes equations without forcing. In both cases the proofs rely on the theory of sectorial operators in which the size of the resolvent has to be estimated, not only in the unstable half-plane, $\mathrm{Re}\,(s) \geqslant 0$, where s is the Laplace transform parameter, but also in sectors of the stable half-plane. Neither Romanov nor Yudovich give a threshold amplitude, one reason being that the authors do not investigate the Reynolds-number dependence of the norm of the resolvent. The latter has recently been investigated for parallel shear flows by Reddy *et al.* (1993) and Trefethen *et al.* (1993). In the latter study it was found that the maximum of the norm of the resolvent in the unstable half-plane for subcritical Reynolds numbers grows like the square of the Reynolds number.

In the present paper some nonlinear stability results for subcritical shear flows are established. This is accomplished by deriving a lower bound on the threshold amplitude for non-vanishing solutions, which is valid for arbitrary forms of the initial disturbances. We use a technique similar to that of Kreiss, Kreiss & Petersson (1992), but extended to three dimensions. They consider nonlinear parabolic, hyperbolic and mixed hyperbolic–parabolic problems in one dimension. For these equations they show that the existence of a bounded resolvent of the linearized operator in the unstable half-plane is sufficient for nonlinear stability, in effect easing the requirement obtained by sectorial operator theory. A bounded resolvent implies an estimate of the solution of the corresponding linear problem on the Laplace transform side. By the Parseval relation this estimate leads to an energy estimate for the linear problem. The energy estimate is then extended to the nonlinear problem. A lower bound for the threshold amplitude also follows.

The presented results are applied to plane Couette flow, for which we calculate the required resolvent estimate numerically. The resulting threshold is compared to an upper bound obtained by numerical simulations. Finally, using a model problem, we discuss various ways to improve the theoretical bound.

2. General threshold bound

For flow in a parallel channel we will in this section derive a lower bound for the amplitude below which all perturbations eventually decay. First the perturbation equation together with suitable norms are introduced. For the straightforward application of the Laplace transform method the equation is written in a form with homogeneous initial conditions. Then we derive a bound of the solution to the linearized problem, theorem 1. The bound is given in terms of the magnitude of the

forcing function and the norm of the resolvent. The resolvent is the Laplace-transformed solution operator to the linearized initial value problem.

Next the linear bound is applied to the nonlinear problem where the nonlinear terms are added to the forcing function, theorem 2. In order that the nonlinear terms should not destroy the bound the solution must be sufficiently small. From this requirement a bound on the threshold amplitude follows. Finally the estimate is applied to the original nonlinear initial value problem, theorems 3 and 4.

2.1. *Notation*

Consider the non-dimensionalized Navier–Stokes equations for incompressible, constant-density flow on some domain D:

$$\left.\begin{aligned} \boldsymbol{u}_t &= R^{-1}\nabla^2\boldsymbol{u} - \boldsymbol{G}(\boldsymbol{u}) - \nabla p, \quad \boldsymbol{x}\in D, \quad t \geqslant 0, \\ \nabla\cdot\boldsymbol{u} &= 0. \end{aligned}\right\} \tag{1}$$

Here $\boldsymbol{u} = (u_1, u_2, u_3)$ are the velocity components in the three space directions, p is the pressure, R is the Reynolds number,

$$\nabla = (\mathrm{D}_1, \mathrm{D}_2, \mathrm{D}_3)^T, \quad \mathrm{D}_i = \partial/\partial x_i,$$

$$\boldsymbol{G}(\boldsymbol{u}) = (\boldsymbol{u}\cdot\nabla)\boldsymbol{u}.$$

We also need initial conditions

$$\boldsymbol{u}(\boldsymbol{x}, 0) = \boldsymbol{f}(\boldsymbol{x}). \tag{2}$$

We will consider the periodic problem where the solution and all data are periodic in the x_1 and the x_3 directions. Let the periodicity be l_1 and l_3, respectively, and introduce

$$D = \{\boldsymbol{x}: -l_1/2 \leqslant x_1 \leqslant l_1/2, \ -1 \leqslant x_2 \leqslant 1, \ -l_3/2 \leqslant x_3 \leqslant l_3/2\} \tag{3}$$

with, possibly moving, solid walls at $x_2 = \pm 1$. In what follows, all estimates are independent of l_1 and l_3, provided they are sufficiently large. Thus all results are valid also for a strip unbounded in the x_1 and x_3 directions. Boundary conditions are

$$\boldsymbol{u}(x_1, -1, x_3, t) = V_{-1}\boldsymbol{e}_1, \quad \boldsymbol{u}(x_1, 1, x_3, t) = V_1\boldsymbol{e}_1. \tag{4}$$

Here $\boldsymbol{e}_i$ is the unit vector in the ith space direction. For the Couette flow example in §3 $V_1 = -V_{-1} = 1$.

We can consider p as a known function of $\boldsymbol{u}$, since

$$\nabla^2 p = -\nabla\cdot\boldsymbol{G}(\boldsymbol{u}). \tag{5}$$

At the solid walls the normal derivative of p must satisfy

$$\mathrm{D}_2 p(x_1, x_2, x_3) = R^{-1}\mathrm{D}_2^2 u_2(x_1, x_2, x_3), \quad x_2 = \pm 1.$$

If the initial data are divergence free, i.e. $\nabla\cdot\boldsymbol{f} = 0$, and the pressure is given by (5), the solutions will continue to be divergence free for all times and we may drop the continuity equation.

Let $\boldsymbol{U}$ and P be a steady solution of (1), and assume the initial condition to be of the form $\boldsymbol{f} = \boldsymbol{U} + \varepsilon\boldsymbol{f}'$, where $\boldsymbol{f}'$ is periodic and $\nabla\cdot\boldsymbol{f}' = 0$. In what follows $\boldsymbol{f}'$ will be normalized such that ε represents a unique perturbation amplitude. Introduce

$$\boldsymbol{u} = \boldsymbol{U} + \varepsilon\boldsymbol{u}', \quad p = P + \varepsilon p_1' + \varepsilon^2 p_2', \tag{6}$$

into (1) and (5), obtaining

$$\boldsymbol{u}_t' = \mathscr{L}\boldsymbol{u}' + \varepsilon\boldsymbol{G}(\boldsymbol{u}') - \varepsilon\nabla p_2'. \tag{7}$$

Here $\mathscr{L}$ is a linear operator, given by

$$\mathscr{L}\boldsymbol{u}' = R^{-1}\nabla^2\boldsymbol{u}' - (U\cdot\nabla)\,\boldsymbol{u}' - (\boldsymbol{u}'\cdot\nabla)\,U - \nabla p_1'$$

and p_1' is defined by

$$\nabla^2 p_1' = -\nabla\cdot(U\cdot\nabla)\,\boldsymbol{u}' - \nabla\cdot(\boldsymbol{u}'\cdot\nabla)\,U,$$
$$\mathrm{D}_2 p_1' = R^{-1}\mathrm{D}_2^2 u_2' \quad \text{at} \quad x_2 = \pm 1.$$

Note that p_1' depends linearly on $\boldsymbol{u}'$. The remaining part of the pressure depends nonlinearly on $\boldsymbol{u}'$ and satisfies

$$\nabla^2 p_2' = -\nabla\cdot\boldsymbol{G}(\boldsymbol{u}'),$$
$$\mathrm{D}_2 p_2' = 0 \quad \text{at} \quad x_2 = \pm 1.$$

Clearly $\boldsymbol{u}'$ will satisfy the following boundary and initial conditions:

$$\boldsymbol{u}'(x_1, -1, x_3, t) = \boldsymbol{u}'(x_1, 1, x_3, t) = 0, \tag{8}$$
$$\boldsymbol{u}'(\boldsymbol{x}, 0) = \boldsymbol{f}'(\boldsymbol{x}). \tag{9}$$

We shall use the usual L_2 scalar product and norm corresponding to twice the perturbation energy,

$$(\boldsymbol{u}, \boldsymbol{v}) = \int_D \boldsymbol{u}\cdot\boldsymbol{v}\,\mathrm{d}\boldsymbol{x}, \quad \|\boldsymbol{u}\|^2 = (\boldsymbol{u}, \boldsymbol{u}).$$

In the estimation of the magnitude of solutions to the Navier–Stokes equations we will use the maximum norm to bound the nonlinear terms. The maximum norm can be related to an L_2 norm containing derivatives through a Sobolev inequality (Kreiss & Lorenz 1989). For our purposes the following form is suitable;

$$|\boldsymbol{u}(\cdot, T)|_\infty^2 \leqslant C_s R^{\frac{3}{2}} \|\boldsymbol{u}(\cdot, T)\|_H^2, \tag{10}$$

where

$$\|\boldsymbol{u}\|_H^2 = \|\boldsymbol{u}\|^2 + R^{-1}J_1^2(\boldsymbol{u}) + R^{-2}(\|\mathrm{D}_1^2\boldsymbol{u}\|^2 + \|\mathrm{D}_3^2\boldsymbol{u}\|^2 + \|\mathrm{D}_1\mathrm{D}_2\boldsymbol{u}\|^2 + \|\mathrm{D}_2\mathrm{D}_3\boldsymbol{u}\|^2), \tag{11}$$

$$J_1^2(\boldsymbol{u}) = \sum_{i=1}^{3} \|\mathrm{D}_i\boldsymbol{u}\|^2. \tag{12}$$

Here C_s does not depend on the periodicity l_1 and l_3 as long as $l_1 \geqslant 1/R^{\frac{1}{2}}$ and $l_3 \geqslant 1/R^{\frac{1}{2}}$.

We want to derive conditions such that the base flow U is stable, i.e.

$$\lim_{t\to\infty} \|\boldsymbol{u}'(\cdot, t)\| = 0, \tag{13}$$

for all R when $R \to \infty$. We shall use the method of Laplace transform. Therefore we transform (7) to a problem with homogeneous initial conditions by introducing

$$\boldsymbol{u}' = \boldsymbol{v} + \mathrm{e}^{-\delta t}\boldsymbol{f}'. \tag{14}$$

Here δ is some positive number. We obtain

$$\left.\begin{aligned} \boldsymbol{v}_t &= \mathscr{L}\boldsymbol{v} + \varepsilon\boldsymbol{G}(\boldsymbol{v} + \mathrm{e}^{-\delta t}\boldsymbol{f}') + \varepsilon\nabla p_2' + \mathrm{e}^{-\delta t}(\mathscr{L} + \delta\boldsymbol{I})\boldsymbol{f}', \\ \boldsymbol{v}(\boldsymbol{x}, 0) &= 0, \end{aligned}\right\} \tag{15}$$

where $\boldsymbol{v}$ satisfies the boundary conditions (8) and p_2' is considered as a function of $\boldsymbol{v}$ using the appropriate Poisson equation. For simplicity we shall first consider

$$\left.\begin{aligned} \boldsymbol{v}_t &= \mathscr{L}\boldsymbol{v} + \varepsilon\boldsymbol{G}(\boldsymbol{v}) + \varepsilon\nabla p_2' + \boldsymbol{F}, \\ \boldsymbol{v}(\boldsymbol{x}, 0) &= 0. \end{aligned}\right\} \tag{16}$$

We assume F and its derivatives are in L_2, and that for some constant $\bar{\gamma} > 0$, independent of R,

$$\lim_{t\to\infty} e^{2\bar{\gamma}t}(\|F(\cdot,t)\|^2 + \|F_t(\cdot,t)\|^2) \to 0. \tag{17}$$

2.2. *Bounds on the linear problem*

We start by considering the linear problem corresponding to (16)

$$\left.\begin{aligned} w_t &= \mathscr{L}w + H(x,t), \\ w(x,0) &= 0. \end{aligned}\right\} \tag{18}$$

Here H has the same properties as F. The Laplace transform of (18) is

$$s\tilde{w} = \mathscr{L}\tilde{w} + \tilde{H}. \tag{19}$$

This equation is known as the resolvent equation, and we assume that the following resolvent condition is satisfied:

$$\|\tilde{w}\|^2 = \|(sI - \mathscr{L})^{-1}\tilde{H}\|^2 \leqslant \kappa(R)\,\|\tilde{H}\|^2, \tag{20}$$

for all s with $\mathrm{Re}(s) \geqslant -\gamma(R)$. Clearly $\kappa \geqslant \|(sI - \mathscr{L})^{-1}\|^2$.

Specifically, we shall consider

$$\|\tilde{w}\| = \|(sI - \mathscr{L})^{-1}\tilde{H}\|^2 \leqslant CR^{\rho}\|\tilde{H}\|^2, \quad \rho > 0, \tag{21}$$

for all s with $\mathrm{Re}(s) \geqslant -\gamma(R)$.

Remark. The case $\rho = 0$ can also be treated. However, some technical details of the proofs will be different.

Remark. If $\gamma \geqslant \gamma_0 > 0$ for all R it is possible to show exponential decay $\sim e^{-\gamma_0 t}$ in (13), independent of R. However, in many cases γ depends on R in such a way that $\gamma \to 0$ when $R \to \infty$. Then the rate of decay will depend on R.

We start with an estimate for the linear problem (18).

THEOREM 1. *Assume there is a constant* $\gamma(R) \in [0, \gamma_1]$ *such that the resolvent condition* (21) *is satisfied for all* s *with* $\mathrm{Re}(s) \geqslant -\gamma$. *Then*

$$e^{2\gamma T}\|w(\cdot,T)\|_{\tilde{H}}^2 + \int_0^T e^{2\gamma t}(\|w(\cdot,t)\|_{\tilde{H}}^2 + \|w_t(\cdot,t)\|_{\tilde{H}}^2)\,dt \leqslant \tfrac{3}{2}e^{2\gamma T}\|H(\cdot,T)\|^2$$

$$+ \tfrac{3}{2}\|H(\cdot,0)\|_{\tilde{H}}^2 + R^{\rho}C_1\|(\delta I + \mathscr{L})\,H(\cdot,0)\|^2, + R^{\rho}C_2\int_0^T e^{2\gamma t}(\|H(\cdot,t)\|^2 + \|H_t(\cdot,t)\|^2)\,dt.$$

Here $\delta = \gamma_1 + 1$ *and* C_1 *and* C_2 *depend on the first and second derivatives of* U *and on the constant* C *in* (21).

The proof of the theorem is given in Appendix A.

Remark. For the right-hand side of the inequality to be bounded for all T we must require that $\bar{\gamma} > \gamma_1$, see (17).

In this theorem the amplitude of the solution to the linear problem is bounded in terms of the forcing function H. Note that for large R the last two terms on the right-hand side of the estimate in theorem 1 are dominant. If one is not interested in the exponential decay rate of the solution w we can consider $\gamma_1 = \gamma = 0$. Then the integral on the left-hand side still remains bounded as $T \to \infty$, ensuring that the solution decays.

2.3. *Bounds on the nonlinear problem*

Now we consider the nonlinear problem (16). To prove all time bounds of the solution we will use a continuation technique, see Kreiss & Lorenz (1989). We shall prove that (16) has a solution satisfying

$$e^{2\gamma T}\|v(\cdot,T)\|_H^2 \leqslant R^\rho K^2, \tag{22}$$

where
$$K^2 = 4\left(C_2\|(\delta I+\mathscr{L})F(\cdot,0)\|^2 + C_2\int_0^\infty e^{2\gamma t}(\|F\|^2+\|F_t\|^2)\,dt\right) \tag{23}$$

for all T, provided ε is sufficiently small. As above $\delta=\gamma_1+1$. Let $\varepsilon>0$ be fixed. Since $v(x,0)=0$ (22) is satisfied in an interval $0\leqslant T\leqslant T_0$, $T_0>0$. Choose T_0 as large as possible, that is (22) holds for all times, or at some time T_0 there is equality in (22). Consider $T\leqslant T_0$. Note that $G(v(\cdot,0))=0$ and $\nabla p_2'(\cdot,0)=0$. Since p_2' satisfies homogeneous boundary conditions, we have by integration by parts

$$\|\nabla p_2'\| \leqslant \|G(v)\|, \quad \|\nabla(p_2')_t\| \leqslant \|G(v)_t\|. \tag{24}$$

By theorem 1 and (24) we have

$$\begin{aligned} e^{2\gamma T}\|v(\cdot,T)\|_H^2 + \int_0^T e^{2\gamma t}(\|v\|_H^2+\|v_t\|_H^2)\,dt &\leqslant \tfrac{3}{2}\|F(\cdot,0)\|_H^2 \\ &+\tfrac{3}{2}e^{2\gamma T}(\|F(\cdot,T)\|^2+2\varepsilon^2\|G(v(\cdot,T))\|^2)+R^\rho C_1\|(\delta I+\mathscr{L})F(\cdot,0)\|^2 \\ &+R^\rho C_2\int_0^T e^{2\gamma t}(\|F\|^2+2\varepsilon^2\|G(v)\|^2+\|F_t\|^2+2\varepsilon^2\|G(v)_t\|^2)\,dt. \end{aligned} \tag{25}$$

By (22) and (10) it follows that

$$\|G(v)\|^2 \leqslant |v|_\infty^2 J_1^2(v) \leqslant R^{\frac{5}{2}+\rho}K^2C_s\|v\|_H^2, \tag{26}$$

$$\|G(v)_t\|^2 \leqslant |v_t|_\infty^2 J_1^2(v)+|v|_\infty^2 J_1^2(v_t) \leqslant 2R^{\frac{5}{2}+\rho}K^2C_s\|v_t\|_H^2. \tag{27}$$

Clearly, if R is sufficiently large then

$$\tfrac{3}{2}e^{2\gamma T}\|F(\cdot,T)\|^2+\tfrac{3}{2}\|F(\cdot,0)\|_H^2 \leqslant \tfrac{1}{8}R^\rho K^2.$$

Thus if
$$4\varepsilon^2R^{2\rho+\frac{5}{2}}K^2C_sC_2 \leqslant 1, \tag{28}$$

then
$$2\varepsilon^2\|G\|^2 \leqslant \tfrac{1}{2}\|v\|_H^2, \quad 2\varepsilon^2\|G_t\|^2 \leqslant \|v_t\|_H^2,$$

and if R is sufficiently large we have

$$e^{2\gamma T}\|v(\cdot,T)\|_H^2 + \int_0^T e^{2\gamma t}\|v\|_H^2\,dt \leqslant \tfrac{3}{4}R^\rho K^2. \tag{29}$$

Clearly there is never equality in (22) which therefore holds for all T. This completes the proof of:

THEOREM 2. *Assume that there is a constant $\gamma(R)\in[0,\gamma_1]$ such that the resolvent condition* (21) *is satisfied for all s with* $\mathrm{Re}\,(s)\geqslant-\gamma$. *If ε satisfies* (28) *then the nonlinear equation* (16) *has a solution satisfying* (29) *for all sufficiently large R. Here K is defined by* (23) *and the constants C_s, C_1 and C_2 are independent of the forcing F and of R.*

Next we shall treat the original problem (7) with inhomogeneous initial conditions. We assume that f' and its derivatives are in L_2. Consider (15) with $\delta=\gamma_1+1$. We normalize the initial condition so that

$$\|(\mathscr{L}+\delta I)f'\|^2 = 1.$$

In this case we can prove an estimate corresponding to (22) with

$$K^2 = 2(C_2(1+\delta^2)+2C_1). \tag{30}$$

As in the proof of theorem 2 we apply theorem 1 to (15) and we can prove the following theorem relating the amplitude of the initial disturbance, ε, to R.

THEOREM 3. *Assume that there is a constant $\gamma(R)\in[0,\gamma_1]$ such that the resolvent condition* (21) *is satisfied for all s with $\mathrm{Re}(s)\geqslant-\gamma$. Then for all normalized initial conditions and all sufficiently large R there is a solution of the nonlinear problem* (7) *that satisfies* (29) *with K defined by* (30), *provided $\varepsilon\leqslant cR^{-\rho-\frac{5}{4}}$. Here c is some number independent of R and of the initial condition.*

The following weaker form of the theorem is useful if we are not interested in the decay rate of the disturbance.

THEOREM 4. *Assume that the resolvent condition* (21) *is satisfied for all s with* $\mathrm{Re}(s)\geqslant 0$. *If*

$$\|(\mathscr{L}+\boldsymbol{I})\varepsilon\boldsymbol{f}'\|\leqslant cR^{-\rho-\frac{5}{4}}$$

and R is sufficiently large then there is a solution of the nonlinear problem (7) *that satisfies* (13). *Here c is some number independent of R and of the initial condition.*

3. Application to plane Couette flow

To apply the theorems derived in the previous section to a specific base flow, a bound of the norm of the resolvent in the unstable half-plane is needed. This quantity must in general be calculated numerically. For plane Couette flow this has been performed by Reddy *et al.* (1993) and Trefethen *et al.* (1993). In this section we show a lower bound for the norm of the resolvent which by comparison to these numerical results proves to be sharp. The value of the norm of the resolvent is then applied to theorem 4 to arrive at a lower bound for the threshold amplitude.

3.1. *The linear initial value problem for parallel shear flows*

The norm of the resolvent can be calculated from the solution of the linear initial value problem

$$\boldsymbol{w}_t = \mathscr{L}\boldsymbol{w}, \quad \boldsymbol{w}(\boldsymbol{x},0) = \boldsymbol{w}_0. \tag{31}$$

cf. (18).

In parallel shear flows $U_i = U(x_2)\,\delta_{1i}$. Expand the solution in a Fourier series

$$w_i = \sum_{m,n} \hat{w}_{i,mn}(x_2)\,\mathrm{e}^{\mathrm{i}(\alpha_m x_1+\beta_n x_3)}, \tag{32}$$

where $\alpha_m = 2\pi m/l_1$ and $\beta_n = 2\pi n/l_3$. In what follows the subscripts for the streamwise and spanwise wavenumbers will be dropped. Using (32), (18) can be reduced to one equation governing the normal velocity ($\hat{w}_2$) and one for the normal vorticity ($\hat{\xi}_2 = \mathrm{i}\beta\hat{w}_1 - \mathrm{i}\alpha\hat{w}_3$). Introducing the vector $\hat{\boldsymbol{q}} = (\hat{w}_2, \hat{\xi}_2)^T$ the linearized equations can be written

$$\frac{\partial\hat{\boldsymbol{q}}}{\partial t} = \hat{\boldsymbol{M}}^{-1}\hat{\boldsymbol{L}}\hat{\boldsymbol{q}}, \quad \hat{\boldsymbol{M}} = \begin{pmatrix} -\mathrm{D}_2^2+k^2 & 0 \\ 0 & 1 \end{pmatrix}, \quad \hat{\boldsymbol{L}} = \begin{pmatrix} \hat{L}_{OS} & 0 \\ -\mathrm{i}\beta\mathrm{D}_2 U & \hat{L}_{SQ} \end{pmatrix}, \tag{33}$$

where

$$\hat{L}_{OS} = -\mathrm{i}\alpha U(-\mathrm{D}_2^2+k^2) - \mathrm{i}\alpha\mathrm{D}_2^2 U - (-\mathrm{D}_2^2+k^2)^2/R, \tag{34a}$$

$$\hat{L}_{SQ} = -\mathrm{i}\alpha U - (-\mathrm{D}_2^2+k^2)/R, \tag{34b}$$

where $k^2 = \alpha^2 + \beta^2$. The solution to (33) can be written formally as

$$\hat{\boldsymbol{q}} = \mathrm{e}^{\hat{\mathscr{L}}t}\hat{\boldsymbol{q}}_0 = \sum_{j=1}^{\infty} \kappa_j \tilde{\boldsymbol{q}}_j \mathrm{e}^{\lambda_j t}, \tag{35}$$

where $\hat{\mathscr{L}} = \hat{\mathscr{L}}_{\alpha,\beta} = \hat{\boldsymbol{M}}^{-1}\hat{\boldsymbol{L}}$ is the Fourier transformed linear evolution operator and $\tilde{\boldsymbol{q}}_j$ and λ_j are its eigenfunctions and eigenvalues, respectively. The eigenvalues consist of both Orr–Sommerfeld and Squire modes. κ_j are the coefficients in the eigenfunction expansion of the initial condition $\hat{\boldsymbol{q}}_0$. This expansion assumes that the eigenvalues are discrete and that the eigenfunctions form a complete set, both of which is true in the Couette flow case (DiPrima & Habetler 1969). The possibility of multiple roots has not been included although they have been found to occur (Gustavsson & Hultgren 1980). However, Reddy & Henningson (1993) have shown that (35) is sufficient in most numerical calculations. Multiple roots will not influence our results.

The energy norm for one Fourier component of the disturbance is

$$\|\hat{\boldsymbol{q}}\|_E^2 = \frac{1}{2k^2}\int_{-1}^{1} \hat{\boldsymbol{q}}^H \hat{\boldsymbol{M}}\hat{\boldsymbol{q}}\,\mathrm{d}x_2 = \frac{1}{2k^2}\int_{-1}^{1} (k^2|\hat{w}_2|^2 + |\mathrm{D}_2\hat{w}_2|^2 + |\hat{\xi}_2|^2)\,\mathrm{d}x_2. \tag{36}$$

The total perturbation energy is recovered if the above expression is summed over all wavenumbers,

$$\tfrac{1}{2}\|\boldsymbol{u}'\|^2 = l_1 l_3 \sum_{m,n} \|\hat{\boldsymbol{q}}_{mn}\|_E^2. \tag{37}$$

If (33) is Laplace transformed one can, with the help of (35), find the following expressions for the resolvent:

$$\tilde{\boldsymbol{q}} = (s\boldsymbol{I} - \hat{\mathscr{L}}_{\alpha,\beta})^{-1}\hat{\boldsymbol{q}}_0 = \sum_{j=1}^{\infty} \frac{\kappa_j}{s-\lambda_j}\tilde{\boldsymbol{q}}_j \tag{38}$$

where s is the Laplace transform variable.

3.2. *Scaled initial value problem*

The Reynolds-number dependence for the norm of the resolvent can be found by rescaling the linearized problem in the same way as Gustavsson (1991) and Reddy & Henningson (1993). If we introduce the new variables

$$t^* = t/R, \quad s^* = sR, \quad \hat{\xi}_2^* = \hat{\xi}_2/\beta R, \quad \hat{w}_2^* = \hat{w}_2 \tag{39}$$

we can rewrite (33) as

$$\frac{\partial \hat{\boldsymbol{q}}^*}{\partial t^*} = \hat{\boldsymbol{M}}^{-1}\hat{\boldsymbol{L}}^*\hat{\boldsymbol{q}}^*, \quad \hat{\boldsymbol{L}}^* = \begin{pmatrix} \hat{L}_{OS}^* & 0 \\ -\mathrm{i}\mathrm{D}_2 U & \hat{L}_{SQ}^* \end{pmatrix}, \tag{40}$$

where $\hat{\boldsymbol{q}}^* = (\hat{w}_2^*, \hat{\xi}_2^*)^T$ and

$$\hat{L}_{OS}^* = -\mathrm{i}\alpha RU(-\mathrm{D}_2^2 + k^2) - \mathrm{i}\alpha R\mathrm{D}_2^2 U - (-\mathrm{D}_2^2 + k^2)^2, \tag{41a}$$

$$\hat{L}_{SQ}^* = -\mathrm{i}\alpha RU - (-\mathrm{D}_2^2 + k^2). \tag{41b}$$

In the scaled equations there are only two independent parameters, αR and k^2, instead of the three originally appearing, α, β and R. In analogy with the above notation we denote $\hat{\mathscr{L}}_{\alpha R,k}^* = \hat{\boldsymbol{M}}^{-1}\hat{\boldsymbol{L}}^*$.

In the new variables the resolvent can be written as

$$\|(s\boldsymbol{I} - \hat{\mathscr{L}}_{\alpha,\beta})^{-1}\|_E = R\|(s^*\boldsymbol{I} - \hat{\mathscr{L}}_{\alpha R,k}^*)^{-1}\|_{E^*} = R\max_{\hat{\boldsymbol{q}}_0^* \neq 0} \frac{\|\tilde{\boldsymbol{q}}^*\|_{E^*}}{\|\tilde{\boldsymbol{q}}_0^*\|_{E^*}}, \tag{42}$$

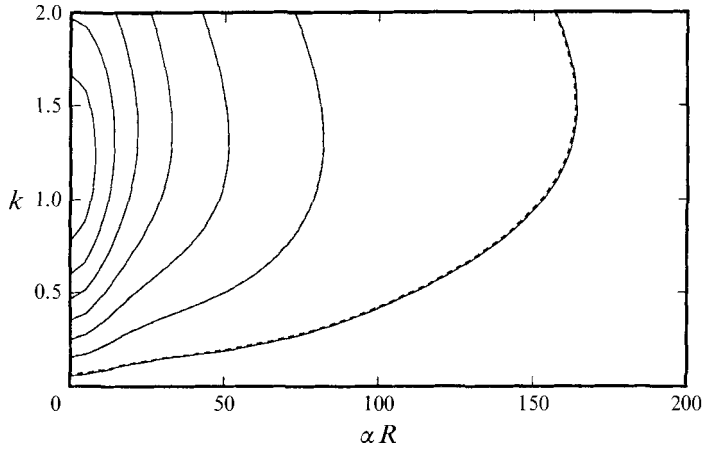

FIGURE 1. $k\|\hat{\mathscr{L}}^{-1}_{\alpha,\beta}\|_E/(\beta R^2)$ for $R = 500$ (solid lines) and $R = 1000$ (dashed lines). The maximum is 0.0152 which occurs at $\alpha R = 0$ and $k = 1.18$. Contour spacing is 0.002.

where $\tilde{\boldsymbol{q}}^*$ is the scaled Laplace-transformed solution. The energy norm becomes

$$\|\tilde{\boldsymbol{q}}^*\|^2_{E^*} = \|\tilde{w}_2^*\|^2_e + \frac{\beta^2 R^2}{2k^2}\|\tilde{\xi}_2^*\|^2 = \frac{1}{2k^2}\int_{-1}^{1}(k^2|\tilde{w}_2^*|^2 + |\mathrm{D}\tilde{w}_2^*|^2)\,\mathrm{d}x_2 + \frac{\beta^2 R^2}{2k^2}\int_{-1}^{1}|\tilde{\xi}_2^*|^2\,\mathrm{d}x_2, \tag{43}$$

where $\|\tilde{w}_2^*\|^2_e$ and $(\beta^2R^2/2k^2)\,\|\tilde{\xi}_2^*\|^2$ are the energies associated with the Laplace-transformed normal velocity and the Laplace-transformed normal vorticity, respectively.

3.3. *The norm of the resolvent for* $\alpha R = 0$

In order to use the general theory to find a bound for the threshold amplitude we need to evaluate the norm of the resolvent in the unstable half-plane $\mathrm{Re}(s^*) \geqslant 0$. For $\alpha R = 0$ the following results holds for the scaled norm of the resolvent.

THEOREM 5. *Let* $\hat{\mathscr{L}}^*_{\alpha R,k} = \hat{\boldsymbol{M}}^{-1}\hat{\boldsymbol{L}}^*$, *where* $\hat{\boldsymbol{M}}$ *and* $\hat{\boldsymbol{L}}$ *are given in* (33) *and* (40). *For* $\alpha R = 0$ *and* $\mathrm{Re}(s^*) \geqslant 0$, $\|(s^*I - \hat{\mathscr{L}}^*_{\alpha R,k})^{-1}\|_{E^*}/R \to C_r > 0$ *as* $R \to \infty$.

Remark. A similar estimate for the norm of the resolvent can be shown for all $\mathrm{Re}(s^*) \geqslant \lambda_1 + C_{s^*}$ where λ_1 is the eigenvalue corresponding to the least damped eigenmode and $C_{s^*} > 0$ and independent of R.

The proof of the theorem can be found in Appendix B.

For plane Couette flow it has been numerically demonstrated that the maximum of the resolvent for $\mathrm{Re}(s)^* \geqslant 0$ occurs for $\alpha R = 0$ at $s^* = 0$ (Trefethen *et al.* 1993). Thus, theorem 5 and (42) imply that the resolvent of the original linearized problem, $\|(s\boldsymbol{I} - \hat{\mathscr{L}}_{\alpha,\beta})^{-1}\|_E$, grows proportionally to R^2 as $R \to \infty$.

We can numerically find the constant multiplying the R^2 dependence of the resolvent. We use a procedure similar to that of Reddy & Henningson (1993). The Orr–Sommerfeld and Squire eigenfunctions for plane Couette flow are first solved for using a Chebyshev method. The norm of the resolvent is then calculated from a truncated version of expansion (38). The result is shown in figure 1 where contours of

$$k\|\hat{\mathscr{L}}^{-1}_{\alpha,\beta}\|_E/\beta R^2$$

are plotted for two Reynolds numbers. The contours coincide for low to moderate αR, showing that the scaling is not only applicable for $\alpha R = 0$ but is also valid

approximately in a region close to the k-axis. The maximum is 0.0152 and occurs on the k-axis, in agreement with results given by Trefethen *et al.* (1993).

Recall that these norms are calculated for particular parameter combinations and that the norm of the resolvent for the full operator in the unstable half-plane is needed in the general theory in order to obtain the bound on the threshold amplitude. This can be found by maximizing the norms calculated above over all values of αR and k or equivalently over all values of α, β. The results above and (37) imply that

$$\max_{\mathrm{Re}(s)\geqslant 0} \|(s\boldsymbol{I}-\mathscr{L})^{-1}\| = R \max_{\mathrm{Re}(s^*)\geqslant 0,\,\alpha R,\,k} \|(s^*\boldsymbol{I}-\hat{\mathscr{L}}^*_{\alpha R,\,k})^{-1}\|_{E^*} = 0.0152R^2. \tag{44}$$

3.4. *Threshold bound*

The result of theorem 4 in the general theory, together with the result (44) implies that

$$\|(\mathscr{L}+\boldsymbol{I})\,\varepsilon \boldsymbol{f}'\| \leqslant cR^{-\frac{21}{4}}, \tag{45}$$

where the initial perturbation is $\varepsilon \boldsymbol{f}$ and c is a number independent of R.

4. Simulation results

The above estimate of the critical amplitude for plane Couette flow is in the form of a lower bound. An upper bound of the critical amplitude can be constructed through an example. To this purpose we present numerical simulation results.

The numerical problem was formulated as follows: find the smallest initial perturbation energy needed to generate solutions which grow to a turbulent amplitude. Since each set of initial data requires a full numerical simulation to determine if it results in a decaying solution or not, an exhaustive search of different shapes of initial data was not feasible. However, results for the Reynolds-number dependence of the critical amplitude for one set of initial data is sufficient as an example and thus to find an upper bound.

The numerical method used to calculate the solutions is described in Appendix C.

4.1. *Domain and initial data*

The size of the domain was chosen as $l_1 = 2\pi$, $l_3 = \pi$, see (3). The initial data used are given by

$$\left.\begin{aligned} \psi &= (1-x_2^2)^2 \sin(2\pi x_3/l_3) \\ (u_1, u_2, u_3) &= \varepsilon(n_1, n_2+\psi_z, n_3-\psi_y). \end{aligned}\right\} \tag{46}$$

Here ε is the amplitude and n_1–n_3 constitutes white noise in the form of Stokes' modes with random phase, the amplitude of which was chosen so that the noise contains 1 % of the total initial perturbation energy. Stokes' modes are the eigenmodes to the flow equations without convective terms. The largest excited wavenumber was 3 in the streamwise direction and 14 in the spanwise direction, and for each wavenumber the 16 least-damped Stokes' modes were used.

This initial velocity field is, apart from the noise, in the form of two streamwise, counter-rotating vortices which span the full channel height.

4.2. *Numerical results*

Figure 2 gives the time history for the perturbation energy for some subcritical and supercritical amplitudes. We see that the subcritical simulations follow qualitatively the linear route of transient growth resulting from the forcing of the streaks by the vortex followed by viscous decay of the energy. For supercritical amplitudes we see four

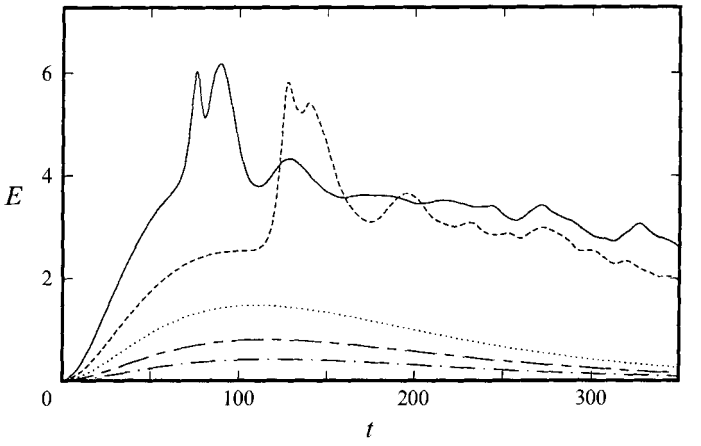

FIGURE 2. Disturbance energy history at Reynolds number 1000 for initial energy density 0.00001 (bottom curve) 0.00002, 0.00004, 0.00008 and 0.00016 (top).

distinct phases: transient growth similar to that for subcritical amplitudes, a rapid secondary instability leading to a transient peak of high amplitude, a similarly rapid decay to a turbulent state and finally irregular amplitude variations as the turbulence relaxes towards a statistically steady state for large times.

The simulations for subcritical amplitudes are here converged to the precision of the graphics with respect to temporal and spatial truncation errors. For the supercritical amplitudes similar convergence is achieved up to and including the transition peak. However, beyond this time the results are not grid-independent. Indeed, because of the positive Lyapunov exponents in this turbulent state, results for different resolutions will start to diverge at some time regardless of how fine the grids are. In any case, experience has shown that the existence of the transition peak at this Reynolds number is sufficient to determine that the solution does not decay.

To find the critical amplitude the simulations were continued until the energy in the wall-normal velocity component rose to turbulent levels, or until a time of about three times that of the first peak in the energy. If turbulence was observed in this time the amplitude was considered supercritical, and otherwise subcritical. In practice the solutions for supercritical amplitudes have a characteristic brief but rapid growth of the perturbation energy giving rise to a high transition peak as seen in figure 2, which makes the determination of critical amplitude unambiguous. The maximum length of the simulation needed to determine the evolution of the solution is proportional to the Reynolds number since the first peak in the energy appears at a time $O(R)$. This value for the time of the maximum was found for linear perturbations lacking streamwise dependence by Gustavsson (1991), and is here found to be valid also for non-sustained nonlinear disturbances.

Note that this procedure gives a critical amplitude which is finite even at or below the critical Reynolds number, since turbulence can develop even in the latter case, although it is not sustained. The issue of determination of the sustainment Reynolds number requires simulations to extremely large times and is outside the scope of the present work. However, for Reynolds numbers somewhat above the sustainment limit, which for plane Couette flow is about 360 (Lundbladh & Johansson 1991; Tillmark & Alfredsson 1992), the determination of the critical amplitude in the way presented is reliable.

Figure 3 gives the critical perturbation energy for different Reynolds numbers. The

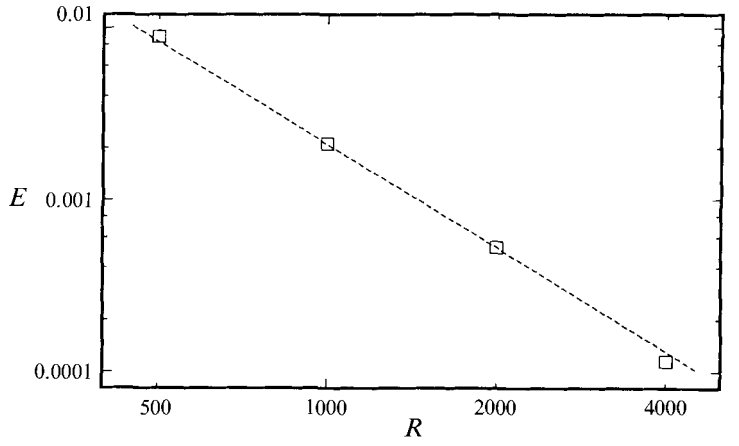

FIGURE 3. The critical perturbation energy as function of Reynolds number. The line is fitted to the data at $R = 2000$ and has slope -2.

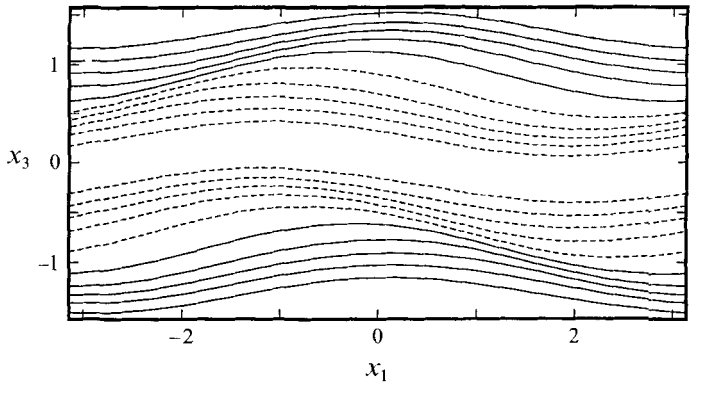

FIGURE 4. The streamwise velocity at the centreline plane $x_2 = 0$ and $t = 115$. Initial energy density is 0.00008. Contour levels start at -0.45, spacing 0.1, with negative contours dashed.

total inaccuracy with respect to temporal and spatial truncation errors, roundoff errors and the amplitude interval between subcritical and supercritical amplitudes is here less than 0.5% up to Reynolds number 2000 and less than 2% at 4000. For the critical perturbation energy the result is $E_{cr} \approx 2000/R^2$ which corresponds to a threshold amplitude

$$\varepsilon_{cr} \sim R^{-1}. \tag{47}$$

When comparing this to (45), ε_{cr} corresponds to $\|\varepsilon \boldsymbol{f}'\|$. We have in this example dealt with a disturbance of constant form when varying the Reynolds number. Thus the same behaviour of the threshold is found for $\|(\mathscr{L}+\boldsymbol{I})\varepsilon \boldsymbol{f}'\|$ apart from the viscous term in $\mathscr{L}$ which contributes a term of order R^{-2}.

The initial growth of this disturbance is a well-known linear effect of forcing of the streamwise velocity by the wall-normal component (Willke 1967; Ellingsen & Palm 1975; Gustavsson 1991; Henningson 1991; Butler & Farell 1992), resulting in streaks of alternating high and low streamwise velocity. The disturbances in the calculations are found to reach an amplitude of order one for all Reynolds numbers before the rapid secondary energy increase sets in.

It is also interesting to briefly consider what effect is responsible for the secondary growth that immediately precedes breakdown to turbulence. Figure 4 shows the streamwise velocity in the centreline plane parallel to the walls for the second highest

amplitude in figure 2 just after the appearance of the secondary instability. The high- and low-speed streaks have started to meander in the spanwise direction. Further study shows that the meandering rapidly increases until the streaks make a maximum angle of about 45° to the mean flow. The streaks then break down and disappear in a few units of time. The meandering appears to be an effect of a secondary instability caused by the large values of spanwise shear between the high- and low-speed streaks as the wave component responsible for the meandering initially decays and only starts growing when the streaks have attained a high amplitude. The spanwise profile of the streamwise velocity is clearly inflexional and although this in itself is not sufficient for instability, the high levels of shear here seem to be the cause of the growing wave, since there are no or only weak inflexions in the wall-normal profile. Further investigation either by linearizing about a state including streaks or by applying dynamical system analysis would certainly be helpful for the understanding of this phenomenon.

4.3. *Influence of the form of initial data*

A number of different initial perturbations were tried in the form of two-dimensional and oblique waves, streamwise vortices, wideband noise and various combinations thereof. For all disturbances involving a streamwise vortex, i.e. with energy in the wall-normal component at zero streamwise wavenumber, the same $O(R^{-1})$ behaviour for the critical amplitude was observed, but at a higher level than the chosen disturbance. Perturbations lacking this energy yielded critical amplitudes which decreased less with increasing Reynolds number.

The noise, when added, serves the purpose of breaking symmetries. Otherwise certain symmetries in the initial data are upheld by the flow equations and can drastically change the result, in general giving an increase of the threshold amplitude. The symmetries which are not broken without noise are two-dimensionality for waves with no variation in the spanwise direction and streamwise independence for vortices and streaks without variation in the streamwise direction. The exact form and amplitude of the noise is found to have negligible effect on the results as long as it is free of symmetries.

Finally, some parameter study was performed for the chosen disturbance. The streamwise period was varied and it was found that lengthening the box would bring down the critical energy density slightly but that the total critical energy would increase due to the larger domain. Similarly a shortening of the box would increase the critical energy but decrease the total critical energy. In both cases this was accompanied by a change in the wavelength of the meandering.

In contrast it was found that both the critical energy density and the total critical energy were higher when the spanwise period was either increased to 4 or decreased to 2 from the present value π at Reynolds number 2000. Thus both the critical perturbation energy and the critical energy density have minima between these values, but naturally do not occur for the same spanwise period.

5. Discussion

In this section we want to discuss the difference between the theoretical threshold bound for Couette flow, which is order $R^{-\frac{21}{4}}$, and the threshold of order R^{-1} found from numerical experiments. We shall first consider a simple example which incorporates a number of essential properties of the Navier–Stokes equations. Although the model problem has not been derived from the Navier–Stokes equations directly, we will give an interpretation of the dependent variables in terms of quantities appearing in the

Navier–Stokes equations. We will also show how to modify the Laplace transform method to get sharp results for the model problem and subsequently discuss its implications for the Navier–Stokes equations.

5.1. *A model problem*

Consider the problem

$$\left.\begin{aligned} \boldsymbol{v}_t &= \boldsymbol{L}\boldsymbol{v}+\boldsymbol{g}(\boldsymbol{v})+\boldsymbol{F}(t), \quad t \geqslant 0, \\ \boldsymbol{v}(0) &= \boldsymbol{f}. \end{aligned}\right\} \tag{48}$$

Here

$$\boldsymbol{L} = \begin{pmatrix} -R^{-1} & 1 & 0 \\ 0 & -R^{-1} & 0 \\ 0 & 0 & -1 \end{pmatrix}, \quad \boldsymbol{v} = \begin{pmatrix} v_1 \\ v_2 \\ v_3 \end{pmatrix}, \quad \boldsymbol{F}(t) = \begin{pmatrix} F_1(t) \\ F_2(t) \\ F_3(t) \end{pmatrix}. \tag{49}$$

Note that the resolvent of the corresponding linear problem satisfies

$$\|(s\boldsymbol{I}-\boldsymbol{L})^{-1}\|^2 \leqslant \|\boldsymbol{L}^{-1}\|^2 \leqslant CR^4 \tag{50}$$

for all s with $\mathrm{Re}\,(s) \geqslant 0$, and that the associated solutions decay as $t \to \infty$, even though they may grow initially. Here $\|\cdot\|$ denotes the usual l_2 norm for matrices.

We shall consider the following nonlinear term:

$$\boldsymbol{g}(\boldsymbol{v}) = \begin{pmatrix} 0 \\ v_3^2 \\ v_1 v_3 \end{pmatrix}. \tag{51}$$

It is clear that the resolvent in this model has the same Reynolds-number dependence as the resolvent of the linear operator in plane Couette flow. The nonlinear term of the model problem also incorporates essential features of the corresponding terms in the Navier–Stokes equations. This will be further discussed below.

By considering the following example we construct an upper bound for the threshold amplitude. Let $\boldsymbol{f} = 0$ and

$$\boldsymbol{F} = \varepsilon h(t) \begin{pmatrix} 1 \\ 1 \\ 1 \end{pmatrix}, \quad h(t) = \begin{cases} 1 & \text{if } t < R \\ 0 & \text{otherwise.} \end{cases}$$

A simple analysis yields that the solution is non-vanishing if

$$\varepsilon > C_F R^{-2}. \tag{52}$$

Note that this corresponds to

$$\int_0^\infty |\boldsymbol{F}|^2 \,\mathrm{d}t > \tilde{C}_F R^{-3}, \tag{53}$$

where $|\cdot|$ is the l_2 norm for vectors. Next we consider (48) with $F = 0$ and initial condition

$$\boldsymbol{f} = \varepsilon \begin{pmatrix} 1 \\ 1 \\ 1 \end{pmatrix}.$$

Similarly the solution is non-vanishing if

$$\varepsilon > C_f R^{-1}. \tag{54}$$

A straightforward application of the Laplace transform method yields the linear estimate

$$|w(T)|^2+\int_0^T |w(t)|^2\,\mathrm{d}t \leqslant (2(\lambda+1)\,\|\boldsymbol{L}^{-1}\|^2+1)\int_0^T |\boldsymbol{H}(t)|^2\,\mathrm{d}t. \tag{55}$$

Here $\boldsymbol{w}$ satisfies the corresponding linear problem with forcing $\boldsymbol{H}(t)$ and homogeneous initial conditions and

$$\frac{(\boldsymbol{u},\boldsymbol{L}\boldsymbol{u})}{|\boldsymbol{u}|^2} \leqslant \lambda,$$

for all vectors $\boldsymbol{u}$. λ is a bound on the numerical range or equivalently a bound on the normalized growth rate.

The nonlinear term satisfies

$$|\boldsymbol{g}(\boldsymbol{v})|^2 \leqslant |\boldsymbol{v}|^4,$$

and as in §2 we apply the linear estimate (55) and derive the following sufficient condition for nonlinear stability, in the case of homogeneous initial condition and a forcing function $\boldsymbol{F}$:

$$\int_0^\infty |\boldsymbol{F}|^2\,\mathrm{d}t \leqslant \tfrac{1}{2}(2(\lambda+1)\,\|\boldsymbol{L}^{-1}\|^2+1)^{-2} = CR^{-8}. \tag{56}$$

Note that there is a discrepancy between this result and the upper bound given by (53). In the case of an inhomogeneous initial condition we introduce

$$\boldsymbol{u} = \boldsymbol{v}+\mathrm{e}^{-t}\boldsymbol{f},$$

and obtain a problem of the above type with forcing $\boldsymbol{F} = \mathrm{e}^{-t}(\boldsymbol{f}+\boldsymbol{L}\boldsymbol{f})$. The Laplace transform method yields the following sufficient condition for stability

$$|\boldsymbol{f}| \leqslant C_2 R^{-4}. \tag{57}$$

Again, there is a discrepancy, cf. (54). Apart from the term $-\frac{5}{4}$, which originates from the Sobolev inequality (10) and the spatial derivative in the nonlinear term, the difference is the same as that found between the theoretical threshold bound (45) and the threshold for the numerical example (47). Thus we have a model problem which behaves essentially the same as the complete problem studied initially.

We shall now improve the results of the Laplace transform method used on the model problem. Consider first the case with homogeneous initial conditions. Note that there are two timescales present. The corresponding linear problem can be separated into two parts with different timescales:

$$\frac{\partial}{\partial t}\begin{pmatrix} w_1 \\ w_2 \end{pmatrix} = \begin{pmatrix} -R^{-1} & 1 \\ 0 & -R^{-1} \end{pmatrix}\begin{pmatrix} w_1 \\ w_2 \end{pmatrix}+\begin{pmatrix} H_1 \\ H_2 \end{pmatrix}, \tag{58}$$

$$\frac{\partial}{\partial t} w_3 = -w_3+H_3. \tag{59}$$

Each part can then be appropriately scaled. In (58) we introduce

$$t^* = R^{-1}t, \quad \boldsymbol{w}^* = \begin{pmatrix} w_1 \\ Rw_2 \end{pmatrix}, \tag{60}$$

yielding

$$\boldsymbol{w}^*_{t^*} = \boldsymbol{L}^*\boldsymbol{w}^*+\boldsymbol{H}^*, \tag{61}$$

$$\boldsymbol{L}^* = \begin{pmatrix} -1 & 1 \\ 0 & -1 \end{pmatrix}, \quad \boldsymbol{H}^* = \begin{pmatrix} RH_1 \\ R^2H_2 \end{pmatrix}. \tag{62}$$

The transformation to $\boldsymbol{w}^*$ corresponds to introducing a weighted norm. We can derive an estimate equivalent to (55) for $\boldsymbol{w}^*$, where

$$\lambda^* \sim 1, \quad \|\boldsymbol{L}^{*-1}\| \sim 1.$$

We derive a similar estimate for w_3 directly. If the linear estimate for w^* is restated in the original scales and the linear estimate for w_3 is added, we have

$$|w_1(T)|^2 + R^2|w_2(T)|^2 + R^{\frac{3}{2}}|w_3(T)|^2 + \int_0^T (R^{-1}|w_1(t)|^2 + R|w_2(t)|^2 + R^{\frac{3}{2}}|w_3(t)|^2)\,\mathrm{d}t$$
$$\leqslant C \int_0^T (R|H_1(t)|^2 + R^3|H_2(t)|^2 + R^{\frac{3}{2}}|H_3(t)|^2)\,\mathrm{d}t. \quad (63)$$

We apply the linear estimate (63) to the nonlinear problem and find that a sufficient condition for stability is

$$\int_0^\infty (R|F_1|^2 + R^3|F_2|^2 + R^{\frac{3}{2}}|F_3|^2)\,\mathrm{d}t \leqslant C.$$

Clearly, by comparison to (53) this is a sharp result for the condition on $\int_0^\infty |\boldsymbol{F}|^2\,\mathrm{d}t$.

In the case of inhomogeneous initial data and $\boldsymbol{F} = 0$ we introduce

$$\boldsymbol{u} = \boldsymbol{v} + \begin{pmatrix} \mathrm{e}^{-t^*} f_1 \\ \mathrm{e}^{-t^*} f_2 \\ \mathrm{e}^{-t} f_3 \end{pmatrix}$$

and obtain a problem of the previous type. A sufficient condition for stability in this case is

$$R^{\frac{1}{4}}|f_1| + R|f_2| + R^{\frac{3}{4}}|f_3| \leqslant C.$$

Again this is a sharp result for the condition on $|\boldsymbol{f}|$, cf. (54).

For initial data the model problem (48) has the same threshold as the numerical simulations in §4 indicated for plane Couette flow. Though the model problem has not been derived from the Navier–Stokes equations directly, it is possible to interpret the dependent variables in (48) as follows: v_1 corresponds to the amplitude of a streamwise streak, i.e. a perturbation in the streamwise velocity with zero streamwise wavenumber; v_2 corresponds to the amplitude of the streamwise vortex driving the streak, i.e. a perturbation in the wall-normal and spanwise velocity at zero streamwise wavenumber. Thus, v_1 and v_2 corresponds to two linear eigenmodes associated with the same wavenumber. Finally, v_3 corresponds to the amplitude of, possibly oblique, waves, i.e. Fourier components with non-zero streamwise wavenumber. Note that the Reynolds-number dependence of the eigenvalues for the streak and the vortex and their linear coupling are also in agreement with those of the linearized Navier–Stokes operator, see e.g. Gustavsson (1991).

The nonlinear terms incorporates some, though not all, of the structure as of the corresponding terms in the Navier–Stokes equations. They are quadratic, and components corresponding to the same wavenumber do not interact nonlinearly. Instead they couple through interactions with other Fourier components. However, the nonlinear terms in the Navier–Stokes equation are energy conserving, a property which is not satisfied by the model. Although this can easily be accomplished by adding further nonlinear terms, see e.g. the model proposed by Henningson & Schmid (1992), we have omitted this in order to simplify the problem. Adding the appropriate terms

does not change the threshold amplitudes and the above method of analysis is applicable. Perhaps surprisingly, this indicates that the energy conservation property is not important for the asymptotic behaviour of the threshold amplitude.

5.2. *Implications for the Navier–Stokes equations*

For the Navier–Stokes equations there are two apparent ways to proceed to derive a sharper bound:

(i) The full equations are written in the form of the linearized problem (33) in the variables w_2 and ξ_2. Let $\boldsymbol{q} = (w_2, \xi_2)^T$; the norm to use with this expansion is then given by

$$\|\boldsymbol{q}\|^2 = \sum_{m,n} \left[R^2 \int_{-1}^{1} \left(|\hat{w}_{2,mn}|^2 + \frac{1}{k_{mn}^2} |\mathrm{D}\hat{w}_{2,mn}|^2 \right) \mathrm{d}x_2 + \frac{1}{k_{mn}^2} \int_{-1}^{1} |\hat{\xi}_{2,mn}|^2 \, \mathrm{d}x_2 \right] \tag{64}$$

with appropriate modifications for $m = n = 0$. Here m, n and k_{mn} are defined as in (32) and (33). When the scaling (39) is applied it is clear that the norm of the resolvent based on (64) for $\alpha R = 0$ is independent of Reynolds number. However, in this case the norm of the resolvent might be larger for $\alpha R \neq 0$. Both the norm and the nonlinear term are in this case most easily defined in Fourier space, which most likely means that the threshold bound must be derived for the transformed equations. Furthermore, in view of the results for the model problem there is little hope that use of this norm alone will be sufficient to find a sharp estimate, since differences in timescales between the modes would most likely also have to be incorporated.

(ii) The original formulation (1) is retained but the norm is replaced by

$$\|\boldsymbol{v}\|^2 = \int_D (v_1^2 + R^r(v_2^2 + v_3^2)) \, \mathrm{d}\boldsymbol{x}, \tag{65}$$

where r is a constant and the time is rescaled as in (39). In principle it is straightforward to evaluate the norm of the resolvent associated with this norm and the results of §2 are then directly applicable. If $r = 2$ this norm is equivalent to the one given above in (i) for $\alpha R = 0$. Since the norm of the resolvent in this case also might be greater when $\alpha R \neq 0$ a lower value of r might give the sharpest bound on the threshold amplitude. Again with reference to the model problem we expect that the components need to be further subdivided to arrive at a sharp result.

A further reason why the theoretical bound is not sharp is that the Sobolev inequality (10) is sharp only for components with small spatial scales. However, the largest linear growth appears for scales of order one or larger. Therefore, it might be necessary to split the dependent variables into two or more scales and to weight the norm for each of these. Another way to proceed here would be to replace the estimate of the nonlinear terms (26) with an expression which is sharp for the relevant scales. A promising route here is to estimate the norm of the quadratic terms by products of higher- but finite-order norms by use of Hölder's inequality. Imbedding theorems then allow estimation of these higher-order norms in terms of the regular L_2 norm.

In future work we hope to improve the theoretical predictions along these lines.

6. Conclusions

A threshold amplitude below which all disturbances regardless of form eventually decay has been derived for a subcritical, bounded, parallel shear flow. Stability was thus proven when the initial perturbation $\boldsymbol{u}$ fulfils $\|\mathscr{L}\boldsymbol{u} + \boldsymbol{u}\|_2 < CR^{-\frac{5}{4}} / \|(\mathscr{L} - s\boldsymbol{I})^{-1}\|^2$. From numerical evaluations of the norm of the resolvent the nonlinear stability of

plane Couette flow was shown when $\|\mathscr{L}\boldsymbol{u}+\boldsymbol{u}\|_2 < cR^{-\frac{21}{4}}$. This constitutes a lower bound on the threshold amplitude. Previous results of similar generality are unknown to the authors, although for plane Couette flow Romanov (1973) has proved that such a threshold amplitude exists without providing an expression for it.

For numerical simulations an upper bound on the threshold amplitude was found to be proportional to R^{-1}. A disturbance in the form of a streamwise vortex pair with a spanwise wavenumber between $\pi/2$ and π and a superimposed low-amplitude wideband noise was found to give the lowest threshold amplitude among the various initial disturbances investigated. The vortices generated streaks of alternating high and low streamwise velocity which broke down from a secondary instability in the form of a rapidly increasing spanwise meandering. The noise here served only as a symmetry breaker to set off the secondary instability and its exact form was found to be unimportant for the result.

The results presented fill a gap in the knowledge of the behaviour of disturbances in the parameter regime between the upper limit of monotonic decay of the energy R_E and the lower limit of linear modal growth R_L. The results are more general than the steady-state solutions found for certain flows in this regime in that they apply to any initial perturbation. We also note that they are applicable to space-periodic and localized disturbances alike. The latter is true as theorems 1–4 give threshold bounds which are uniformly valid with respect to the spatial period l_1 and l_3, i.e. they are also valid for an infinite strip.

It was further demonstrated how the theoretical results can be improved by reverting to other norms than that corresponding to the disturbance energy. This was accomplished by rescaling of certain components of the flow field and by rescaling of the time for some components so that the scaled time for the linear behaviour was order one. Besides the improvement of the bound, the scaled norms may provide additional understanding of the transition process by assessing the relative importance of different components of the initial disturbance.

Similar results can be derived whenever a bound on the norm of the resolvent exists, for example for plane Poiseuille flow below the critical Reynolds number for modal growth. The results may also be extended to other bounded geometries such as Hagen–Poiseuille and Taylor–Couette flow although the technique in the proof of theorems 1–4 has to be adapted. For shear flows in unbounded domains, e.g. boundary layers, the norm of the resolvent is in general unbounded, precluding the straightforward application of the presented theory. However, if it is assumed that the most critical disturbance has support only in a bounded domain, a model problem with a restricted domain is pertinent. For this model a lower bound on the threshold can be constructed, again provided the Reynolds number is subcritical. A further complication in the boundary-layer geometry is how to incorporate the non-parallel effects.

Whereas the lower bound on the threshold amplitude in its present form is not a sharp result, its mere existence and reasonable magnitude justifies a search for the threshold amplitude and corresponding critical disturbance by experimental or numerical techniques.

We wish to thank Heinz-Otto Kreiss for fruitful discussions on the topic of nonlinear stability. We also thank Satish Reddy and Arne Johansson for careful proofreading and for suggesting improvements. We gratefully acknowledge financial support from the Göran Gustafsson Foundation, the Swedish National Board for Industrial and Technical Development (NUTEK), The Swedish Research Council for Engineering Sciences (TFR) and the Aeronautical Research Institute of Sweden (FFA).

Supercomputer time was provided by the National Center for Supercomputer Applications (NCSA), Urbana, Illinois.

Appendix A. Proof of theorem 1

First we prove two lemmata.

LEMMA 1. *Assume that there is a constant* $\gamma(R) \in [0, \gamma_1]$ *such that the resolvent condition* (20) *is satisfied for all* s *with* $\mathrm{Re}(s) \geqslant -\gamma$. *Then*

$$\|\tilde{w}\|_H^2 \leqslant \tilde{C}_2 R^\rho \|\tilde{H}\|^2, \tag{A 1}$$

for all s *with* $\mathrm{Re}(s) \geqslant -\gamma$. *Here* $\tilde{C}_2$ *depends on the first and second derivatives of* U *and on the constant* C *in* (21).

Proof. Multiply (19) by $\tilde{w}$ and integrate. After partial integration we obtain

$$R^{-1} J_1^2(\tilde{w}) = -\mathrm{Re}(s)\,\|\tilde{w}\|^2 + \mathrm{Re}(\tilde{w}, (U\cdot\nabla)\,\tilde{w} + \boldsymbol{B}\tilde{w} + \nabla\tilde{p}_1) + \mathrm{Re}(\tilde{w}, \tilde{H}).$$

Note that $-\mathrm{Re}(s) \leqslant \gamma_1$ and $B\tilde{w} = (\tilde{w}\cdot\nabla)\,U$. By partial integration it follows that

$$(\tilde{w}, (U\cdot\nabla)\,\tilde{w}) = 0, \quad (\tilde{w}, \nabla\tilde{p}_1) = 0.$$

Note that all boundary terms vanish since $\tilde{w}$ vanishes at the walls. Hence

$$\|\tilde{w}\|^2 + R^{-1} J_1^2(\tilde{w}) \leqslant \tilde{C}_1 R^\rho \|\tilde{H}\|^2.$$

Here $\tilde{C}_1$ depends on the first derivatives of U and on the constant in (21). Next we differentiate (19) with respect to x_1. As above we obtain after partial integration

$$\begin{aligned} R^{-1}(\|\mathrm{D}_1^2\tilde{w}\|^2 + \|\mathrm{D}_1\mathrm{D}_2\tilde{w}\|^2 + \|\mathrm{D}_1\mathrm{D}_3\tilde{w}\|^2) \\ = -\mathrm{Re}(s)\,\|\mathrm{D}_1\tilde{w}\|^2 - \mathrm{Re}((\mathrm{D}_1\tilde{w}, (\mathrm{D}_1 U\cdot\nabla)\,\tilde{w}) + (\mathrm{D}_1\tilde{w}, \mathrm{D}_1 B\tilde{w}) + (\mathrm{D}_1^2\tilde{w}, \tilde{H})). \end{aligned}$$

Since we have differentiated in a direction tangential to the wall all boundary terms appearing after partial integration vanish. We can estimate the right-hand side in terms of $\|\tilde{w}\|^2$, $J_1^2(\tilde{w})$ and $\|\tilde{H}\|^2$. By differentiating in the other tangential direction, x_3, we obtain a corresponding result and the lemma follows.

LEMMA 2. *Assume that there is a constant* $\gamma(R) \in [0, \gamma_1]$ *such that the resolvent condition* (20) *is satisfied for all* s *with* $\mathrm{Re}(s) \geqslant -\gamma$. *Then*

$$\begin{aligned} \mathrm{e}^{2\gamma T}(\|w(\cdot,T)\|^2 + R^{-1}\|\mathrm{D}_1 w(\cdot,T)\|^2 + R^{-1}\|\mathrm{D}_3 w(\cdot,T)\|^2) + \int_0^T \mathrm{e}^{2\gamma t}\|w(\cdot,t)\|_{\tilde{H}}^2\,\mathrm{d}t \\ \leqslant \tilde{C}_3 R^\rho \int_0^T \mathrm{e}^{2\gamma t}\|H(\cdot,t)\|^2\,\mathrm{d}t. \end{aligned}$$

Here $\tilde{C}_3$ *depends on the first and second derivatives of* U *and on the constant* C *in* (20).

Proof. By lemma 1 and the Parseval relation it follows that for any $\eta \geqslant -\gamma$

$$\int_0^T \mathrm{e}^{-2\eta t}\|w\|_{\tilde{H}}^2\,\mathrm{d}t \leqslant \int_0^\infty \mathrm{e}^{-2\eta t}\|w\|_{\tilde{H}}^2\,\mathrm{d}t \leqslant C_2 R^\rho \int_0^\infty \mathrm{e}^{-2\eta t}\|H\|^2\,\mathrm{d}t.$$

Since for $t \leqslant T$ the solution does not depend on function values $H(\cdot,t)$ where $t > T$ we can in the above inequality assume $H \equiv 0$ for $t > T$. Let $\eta = -\gamma$ and we have

$$\int_0^T \mathrm{e}^{2\gamma t}\|w\|_{\tilde{H}}^2\,\mathrm{d}t \leqslant \tilde{C}_2 R^\rho \int_0^T \mathrm{e}^{2\gamma t}\|H\|^2\,\mathrm{d}t. \tag{A 2}$$

Multiply (18) by w and integrate. As in lemma 1 integration by parts yields

$$\frac{1}{2}\frac{\mathrm{d}}{\mathrm{d}t}\|w\|^2 + R^{-1}J_1^2(w) \leqslant (|B|_\infty + \tfrac{1}{2})\,\|w\|^2 + \tfrac{1}{2}\|H\|^2, \tag{A 3}$$

where $|\boldsymbol{B}|_\infty = \max_{x\in D}\|\boldsymbol{B}\|_2$. Consider (18) differentiated with respect to x_1 and x_3. Similarly we obtain

$$\frac{1}{2}\frac{\mathrm{d}}{\mathrm{d}t}(\|\mathrm{D}_1 w\|^2 + \|\mathrm{D}_3 w\|^2) + \tfrac{1}{2}R^{-1}(\|\mathrm{D}_1^2 v\|^2 + \|\mathrm{D}_1\mathrm{D}_2 w\|^2 + \|\mathrm{D}_2\mathrm{D}_3 w\|^2 + \|\mathrm{D}_3^2 w\|^2)$$
$$\leqslant \tilde{C}_4(J_1^2(w) + \|w\|^2) + \tfrac{1}{2}R\|H\|^2. \tag{A 4}$$

Here $\tilde{C}_4$ depends on the first and second derivatives of U. Thus

$$\frac{\mathrm{d}}{\mathrm{d}t}(\mathrm{e}^{2\gamma t}(\|w\|^2 + R^{-1}\|\mathrm{D}_1 w\|^2 + R^{-1}\|\mathrm{D}_3 w\|^2))$$
$$\leqslant \tilde{C}_5(\mathrm{e}^{2\gamma t}\|w\|^2 + R^{-1}J_1^2(w)) + 2\mathrm{e}^{2\gamma t}\|H\|^2. \tag{A 5}$$

Integrate (A 5) from 0 to T, combine the result with (A 2) and the lemma follows.

Proof of theorem 1. By (A 3) and (A 4) we have

$$R^{-1}\,\mathrm{e}^{2\gamma t}J_1^2(w) \leqslant \mathrm{e}^{2\gamma t}((|\boldsymbol{B}|_\infty + \tfrac{1}{2})\,\|w\|^2 + \tfrac{1}{2}\|H\|^2 + \|w_t\|\,\|w\|), \tag{A 6}$$

$$R^{-2}\,\mathrm{e}^{2\gamma t}(\|\mathrm{D}_1^2 w\|^2 + \|\mathrm{D}_1\mathrm{D}_2 w\|^2 + \|\mathrm{D}_2\mathrm{D}_3 w\|^2 + \|\mathrm{D}_3^2 w\|^2)$$
$$\leqslant \mathrm{e}^{2\gamma t}(2\tilde{C}_4 R^{-1}(J_1^2(w) + \|w\|^2) + \|H\|^2 + 2R^{-1}(\|\mathrm{D}_1 w_t\|\,\|\mathrm{D}_1 w\| + \|\mathrm{D}_3 w_t\|\,\|\mathrm{D}_3 w\|)). \tag{A 7}$$

To estimate the time derivatives of w we differentiate (18) with respect to t. Clearly w_t satisfies (18) with forcing H_t and initial condition $w_t(x,0) = H(x,0)$. After a transformation of type (14) with $\delta = \gamma_1 + 1$ we can apply lemma 2 obtaining

$$\mathrm{e}^{2\gamma T}(\|w_t\|^2 + R^{-1}\|\mathrm{D}_1 w_t\|^2 + R^{-1}\|\mathrm{D}_3 w_t\|^2) + \int_0^T \mathrm{e}^{2\gamma t}\|w_t\|_{\tilde{H}}^2\,\mathrm{d}t$$
$$\leqslant R^\rho\frac{\tilde{C}_3}{2}\,\|(\delta\boldsymbol{I} + \boldsymbol{L})\,H(\cdot,0)\|^2 + \tfrac{3}{2}\|H(\cdot,0)\|_{\tilde{H}}^2 + R^\rho\tilde{C}_3\int_0^T \mathrm{e}^{2\gamma t}\|H_t\|^2\,\mathrm{d}t. \tag{A 8}$$

Combine (A 8), (A 6), (A 7) and lemma 2 applied to w, and the theorem follows.

Appendix B. Proof of theorem 5

For $\alpha R = 0$ the individual operators $\hat{\mathscr{L}}_{OS}^* = \hat{\boldsymbol{M}}^{-1}\hat{L}_{OS}^*$ and $\hat{\mathscr{L}}_{SQ}^* = \hat{\boldsymbol{M}}^{-1}\hat{L}_{SQ}^*$ are normal, i.e. they commute with their adjoints. For a normal operator, the norm of the resolvent can be calculated (Kato 1976):

$$\|(s\boldsymbol{I} - \mathscr{L})^{-1}\| = \frac{1}{\mathrm{dist}\,\{s, \Lambda\}}, \tag{B 1}$$

where Λ is the set of eigenvalues of $\mathscr{L}$ and $\mathrm{dist}\,\{s,\Lambda\}$ denotes the distance between s and the closest eigenvalue in the set Λ.

The eigenvalues of the scaled operators are

$$\lambda_j^{*OS} = -\frac{1}{2k^2}\int_{-1}^{1}(|\mathrm{D}_2^2\tilde{w}_{2,j}^*|^2 + 2k^2|\mathrm{D}_2\tilde{w}_{2,j}^*|^2 + k^4|\tilde{w}_{2,j}^*|^2)\,\mathrm{d}x_2, \tag{B 2a}$$

$$\lambda_j^{*SQ} = -\frac{1}{2k^2}\int_{-1}^{1}(|\mathrm{D}_2\tilde{\xi}_{2,j}^*|^2 + k^2|\tilde{\xi}_{2,j}^*|^2)\,\mathrm{d}x_2, \tag{B 2b}$$

where $\tilde{w}_{2,j}^*$ and $\tilde{\xi}_{2,j}^*$ are eigenfunctions of the scaled Orr–Sommerfeld and Squire

operators, normalized such that $\|\tilde{w}_2^*\|_e = 1$ and $\|\tilde{\xi}_2^*\| = 1$. The eigenvalues are ordered such that the damping rates increase with j.

Since both the Orr–Sommerfeld and Squire eigenvalues for the scaled problem at $\alpha R = 0$ are real and negative, the square of the shortest distances to the two spectra from a point in the unstable half-plane are $(\lambda_1^{*OS} - s_r^*)^2 + s_i^{*2}$ and $(\lambda_1^{*SQ} - s_r^*)^2 + s_i^{*2}$, respectively, where $s_r^* = \mathrm{Re}(s^*)$ and $s_i^* = \mathrm{Im}(s^*)$. From the component form of the Laplace transform of the scaled version of the initial value problem one finds

$$\|\tilde{w}_2^*\|_e^2 \leqslant \|(s^* I - \hat{\mathscr{L}}_{OS}^*)^{-1}\|_e^2 \, \|\hat{w}_2^*(0)\|_e^2 = \frac{1}{(\lambda_1^{*OS} - s_r^*)^2 + s_i^{*2}} \|\hat{w}_2^*(0)\|_e^2, \tag{B 3a}$$

$$\begin{aligned} \|\hat{\xi}_2^*\|^2 &\leqslant \|(s^* I - \hat{\mathscr{L}}_{SQ}^*)^{-1}\|^2 [\|\tilde{w}_2^* \, \mathrm{D}_2 \, U\|^2 + \|\hat{\xi}_2^*(0)\|^2] \\ &\leqslant \frac{1}{(\lambda_1^{*SQ} - s_r^*)^2 + s_i^{*2}} [2|\mathrm{D}_2 \, U_{max}|^2 \, \|\tilde{w}_2^*\|_e^2 + \|\hat{\xi}_2^*(0)\|^2]. \end{aligned} \tag{B 3b}$$

Substituting into (42) yields

$$\begin{aligned} \|(s^* I - \hat{\mathscr{L}}_{\alpha R, k}^*)^{-1}\|_{E^*}^2 &\leqslant \max_{\|\hat{q}_0^*\| \neq 0} \frac{1}{(\delta + s_r^*)^2 + s_i^{*2}} \\ &\quad \times \left[1 + \frac{2k^{-2}\beta^2 R^2 |\mathrm{D}_2 \, U_{max}|^2 \, \|\hat{w}_2^*(0)\|_e^2}{((\delta + s_r^*)^2 + s_i^{*2})(\|\hat{w}_2^*(0)\|_e^2 + \beta^2 R^2 \|\hat{\xi}_2^*(0)\|^2)}\right] \\ &\leqslant \frac{1}{(\delta + s_r^*)^2 + s_i^{*2}} \left[1 + \frac{2k^{-2}\beta^2 R^2 |\mathrm{D}_2 \, U_{max}|^2}{(\delta + s_r^*)^2 + s_i^{*2}}\right], \end{aligned} \tag{B 4}$$

where $\delta = \min\{|\lambda_1^{*OS}|, |\lambda_1^{*SQ}|\}$.

The above expression grows like R^2 as R becomes large. This implies that the norm of the resolvent for the scaled problem cannot grow faster than R as $R \to \infty$. By introducing (43) into (42) and choosing $\|\xi^*(0)\| = 0$ it is easily verified that this result is sharp. Thus, the norm of the resolvent grows proportionally to R as $R \to \infty$ for $\alpha R = 0$. This completes the proof of theorem 5.

The right-hand side of (B 4) has a maximum for $s = 0$. This does not prove that the norm of the resolvent has a maximum for that s since (B 4) is an inequality. The numerical calculations of Trefethen *et al.* (1993) referred to above, however, show that the maximum is indeed at that position.

Appendix C. Numerical simulation method and error estimates

A spectral method was employed to solve the incompressible Navier–Stokes equations, with Fourier representation in the streamwise and spanwise directions, and Chebyshev polynomials in the wall-normal direction. The nonlinear terms are treated pseudo-spectrally using FFTs, in a manner similar to that of Kim, Moin & Moser (1987), although here instead of the variables themselves, their second derivatives are expanded in Chebyshev series (Greengard 1991). This results in better numerical accuracy since the need for the evaluation of ill-conditioned Chebyshev derivatives is virtually eliminated. The time advancement used was a third-order Runge–Kutta method for the nonlinear terms and a second-order Crank–Nicholson method for the linear terms, with a time step dynamically kept at 90% of the theoretical CFL limit. Aliasing errors from the evaluation of the nonlinear terms were removed by the $\frac{3}{2}$-rule when the horizontal FFTs were calculated. The complete numerical method for the channel flow geometry is described in Lundbladh, Henningson & Johansson (1992). The code has previously been used in e.g. the study of Lundbladh & Johansson (1991).

Amplitude	Reynolds number	Low resolution	High resolution
Critical	500	$16 \times 49 \times 16$	$24 \times 65 \times 24$
Critical	1000	$8 \times 49 \times 16$	$12 \times 65 \times 24$
Critical	2000	$8 \times 49 \times 24$	$12 \times 65 \times 32$
Critical	4000	$8 \times 49 \times 24$	$12 \times 65 \times 32$
Subcritical	1000	$8 \times 49 \times 16$	$12 \times 65 \times 24$
Supercritical	1000	$24 \times 65 \times 24$	$32 \times 81 \times 32$

TABLE 1. Numerical resolution for different physical parameters: number of spectral modes used in, respectively, the streamwise, wall-normal and spanwise directions

All numerical results presented have been checked for effects of finite resolution by repeating the simulations with identical data but with lower resolution in all spatial directions and time. Table 1 gives the resolution for each of the simulations. The four first rows refer to the determination of the critical amplitude and the last two to the simulations for results shown in figures 2 and 4. The numerical error was taken as the difference between the result from the high and the low resolution, while the results presented are from the high resolution runs throughout. The roundoff error was checked for the determination of the critical amplitude at the highest Reynolds number by comparing to a simulation with one bit truncated in all of the elementary operations.

REFERENCES

BUTLER, K. M. & FARRELL, B. F. 1992 Three-dimensional optimal perturbations in viscous shear flow. *Phys. Fluids* A **4**, 1637–1650.

COWLEY, S. J. & SMITH, F. T. 1985 On the stability of Poiseuille–Couette flow: a bifurcation from infinity. *J. Fluid Mech.* **156**, 83–100.

DAVIS, S. H. 1969 Buoyancy-surface tension instability by the method of energy. *J. Fluid Mech.* **39**, 347–359.

DIPRIMA, R. C. & HABETLER, G. J. 1969 A completeness theorem for non-selfadjoint eigenvalue problems in hydrodynamic stability. *Arch. Rat. Mech. Anal.* **32**, 218–227.

EHRENSTEIN, U. & KOCH, W. 1991 Three-dimensional wavelike equilibrium states in plane Poiseuille flow. *J. Fluid Mech.* **228**, 111–148.

ELLINGSEN, T. & PALM, E. 1975 Stability of linear flow. *Phys. Fluids* **18**, 487–488.

GALDI, G. P. & STRAUGHAN, B. 1985 Exchange of stabilities, symmetry, and nonlinear stability. *Arch. Rat. Mech. Anal.* **89**, 211–228.

GOR'KOV, L. P. 1957 Stationary convection in a plane liquid layer near the critical heat transfer point. *Zh. Eksp. Teor. Fiz.* **33**, 402–407. (Translated in *Sov. Phys. JETP* **6**, 311–315 (1958).)

GREENGARD, L. 1991 Spectral integration and two-point boundary value problems. *SIAM J. Numer. Anal.* **28**, 1071–1080.

GROHNE, D. 1969 Die Stabilität der ebenen Kanalströmung gegenüber dreidimensionalen Störungen von endlicher Amplitude. *AVA Göttingen Rep.* 69 A 30.

GUSTAVSSON, L. H. 1991 Energy growth of three-dimensional disturbances in plane Poiseuille flow. *J. Fluid Mech.* **224**, 241–260.

GUSTAVSSON, L. H. & HULTGREN, L. S. 1980 A resonance mechanism in plane Couette flow. *J. Fluid Mech.* **98**, 149–159.

HENNINGSON, D. S. 1991 An eigenfunction expansion of localized disturbances. In *Advances in Turbulence 3* (ed. A. V. Johansson & P. H. Alfredsson), pp. 162–169. Springer.

HENNINGSON, D. S., LUNDBLADH, A. & JOHANSSON, A. V. 1993 A mechanism for bypass transition from localized disturbances in wall-bounded shear flows. *J. Fluid Mech.* **250**, 169–207.

HENNINGSON, D. S. & SCHMID, P. J. 1992 Vector eigenfunction expansions for plane channel flows. *Stud. Appl. Maths* **87**, 15–43.

HERBERT, T. 1983 On perturbation methods in nonlinear stability theory. *J. Fluid Mech.* **126**, 167–186.

HERRON, I. H. 1991 Observations on the role of vorticity in the stability of wall bounded flows. *Stud. Appl. Maths* **85**, 269–286.

JOSEPH, D. D. 1965 On the stability of the Boussinesq equations. *Arch. Rat. Mech. Anal.* **20**, 59–71.

JOSEPH, D. D. 1966 Nonlinear stability of the Boussinesq equations by the energy method. *Arch. Rat. Mech. Anal.* **22**, 163–184.

JOSEPH, D. D. 1976 *Stability of Fluid Motions I.* Springer.

KATO, T. 1976 *Perturbation Theory for Linear Operators.* Springer.

KIM, J., MOIN, P. & MOSER, R. 1987 Turbulence statistics in fully developed channel flow. *J. Fluid Mech.* **177**, 133–166.

KREISS, G., KREISS, H.-O. & PETERSSON, N. A. 1992 On the convergence to steady state of solutions of nonlinear hyperbolic-parabolic systems. *TRITA-NA* 9221. Royal Institute of Technology, Stockholm, Sweden.

KREISS, H.-O. & LORENZ, J. 1989 *Initial-Boundary Value Problems and the Navier–Stokes Equations.* Academic.

LUNDBLADH, A., HENNINGSON, D. S. & JOHANSSON, A. V. 1992 An efficient spectral integration method for the solution of the Navier–Stokes equations. *FFA-TN* 1992-28. Aeronautical Research Institute of Sweden, Bromma.

LUNDBLADH, A. & JOHANSSON, A. V. 1991 Direct simulation of turbulent spots in plane Couette flow. *J. Fluid Mech.* **229**, 499–516.

MALKUS, W. V. R. & VERONIS, G. 1958 Finite amplitude cellular convection. *J. Fluid Mech.* **4**, 225–260.

MEKSYN, D. & STUART, J. T. 1951 Stability of viscous motion between parallel planes for finite disturbances. *Proc. R. Soc. Lond.* A **208**, 517–526.

NAGATA, M. 1990 Three-dimensional finite-amplitude solutions in plane Couette flow: bifurcation from infinity. *J. Fluid Mech.* **217**, 519–527.

ORR, W. M. F. 1907 The stability or instability of the steady motions of a perfect liquid and of a viscous liquid. Part I: A perfect liquid. Part II: A viscous liquid. *Proc. R. Irish Acad.* A **27**, 9–138.

REDDY, S. C. & HENNINGSON, D. S. 1993 Energy growth in viscous channel flows. *J. Fluid Mech.* **252**, 209–238.

REDDY, S. C., SCHMID, P. J. & HENNINGSON, D. S. 1993 Pseudospectra of the Orr–Sommerfeld operator. *SIAM J. Appl. Maths* **53**, 15–47.

REYNOLDS, O. 1895 On the dynamical theory of incompressible viscous fluids and the determination of the criterion. *Phil. Trans. R. Lond. Soc.* A **186**, 123–164.

ROMANOV, V. A. 1973 Stability and plane-parallel Couette flow. *Funkcional Anal. i Prolożen.* **7**(2), 72–73. (Translated in *Functional Anal. Applics.* **7**, 137–146 (1973).)

SCHMID, P. J. & HENNINGSON, D. S. 1992 A new mechanism for rapid transition involving a pair of oblique waves. *Phys. Fluids* A **4**, 1986–1989.

SERRIN, J. 1959 On the stability of viscous fluid motions. *Arch. Rat. Mech. Anal.* **3**, 1–13.

STUART, J. T. 1960 On the nonlinear mechanics of wave disturbances in stable and unstable parallel flows. Part 1. The basic behaviour in plane Poiseuille flow. *J. Fluid Mech.* **9**, 353–370.

TILLMARK, N. & ALFREDSSON, P. H. 1992 Experiments on transition in plane Couette flow. *J. Fluid Mech.* **235**, 89–102.

TREFETHEN, L. N., TREFETHEN, A. E., REDDY, S. C. & DRISCOLL, T. A. 1993 Hydrodynamic stability without eigenvalues. *Science* **261**, 578–584.

WATSON, J. 1960 On the nonlinear mechanics of wave disturbances in stable and unstable parallel flows. Part 2. The development of a solution for plane Poiseuille and for plane Couette flow. *J. Fluid Mech.* **9**, 371–389.

WILLKE, L. H. 1967 Stability in time-symmetric flows. *J. Math. Phys.* **46**, 151–163.

YUDOVICH, V. I. 1989 *The Linearization Method in Hydrodynamical Stability Theory.* American Mathematical Society.

ZAHN, J. P., TOOMRE, J., SPIEGEL, E. A. & GOUGH, D. O. 1974 Nonlinear cellular motions in Poiseuille channel flow. *J. Fluid Mech.* **64**, 319–345.